Fast Implementation of Scale-Space by Interpolatory Subdivision Scheme

Yu-Ping Wang and Ruibin Qu

Abstract—While the scale-space approach has been widely used in computer vision, there has been a great interest in fast implementation of scale-space filtering. In this paper, we introduce an interpolatory subdivision scheme (ISS) for this purpose. In order to extract the geometric features in a scale-space representation, discrete derivative approximations are usually needed. Hence, a general procedure is also introduced to derive exact formulae for numerical differentiation with respect to this ISS. Then, from ISS, an algorithm is derived for fast approximation of scale-space filtering. Moreover, the relationship between the ISS and the Whittaker-Shannon sampling theorem and the commonly used spline technique is discussed. As an example of the application of ISS technique, we present some examples on fast implementation of $\lambda\tau$-spaces as introduced by Gökmen and Jain [12], which encompasses various famous edge detection filters. It is shown that the ISS technique demonstrates high performance in fast implementation of the scale-space filtering and feature extraction.

Index Terms—Scale-space, interpolatory subdivision scheme, B-splines, edge detection, image representation.

1 Introduction

MULTISCALE or multiresolution description of signals has been playing a very important role since the introduction of the Gaussian scale-space filtering by Witkin [1]. In particular, the pyramid algorithm in recent wavelet models aims at representing image copies at multiple resolutions efficiently. There has been great interest in the efficient representation of image structures, which is very useful for high level visual processing tasks such as object recognition and image segmentation.

In the past few years, various powerful mathematical methods have been developed for successive refinements of image structures. Among them, the B-spline technique is a frequently used one which can implement the Gaussian scale-space filtering efficiently [2], [3]. In fact, B-spline technique is one type of subdivision algorithms which provides an efficient tool for the description of image structures [4], [5].

In this paper, an interpolatory subdivision scheme (ISS) is introduced for the efficient implementation of scale-space representation. ISS has been intensively studied in the areas of CAGD and wavelet construction. For example, the famous Daubechies wavelet can be derived from interpolatory subdivisions [6]. It was also used successfully for surface interpolation [7], [8], [9], [10] and for solving two-point boundary value problems [11]. In this paper, we apply this approach for efficient implementation of scale-space filtering. As a specific example, we discuss how it can be used for fast realization of $\lambda\tau$-space representation introduced in [12], which includes some famous edge detection filters, such as Marr-Hilderth edge detector [13], Canny edge detector [14], the first-and second-order R-filters, Deriche's detector, Sarkar and Boyer's edge detector, Shen and Castan's edge detector. In order to extract the differential geometric structure, the differential operators are usually needed. Therefore, a general procedure is also introduced to compute the derivatives of the interpolatory basis with respect to this ISS. Finally, the relations between the ISS and the Shannon sampling basis and the spline approach are discussed. It can be shown that the ISS is an efficient approach for multiresolution image analysis.

2 An Interpolatory Subdivision Scheme for Curves

2.1 Definitions of the Subdivision Schemes

A uniform subdivision or binary subdivision scheme is defined as follows: Suppose that the initial *control points* in $\mathbf{R}^3$ (or in $\mathbf{R}^d$, $d \geq 1$) are denoted by $\mathbf{P}_i^0$, $i \in \mathbb{Z}$, then the refined control points $\{\mathbf{P}_i^{k+1}, i \in \mathbb{Z}\}$ are obtained from $\{\mathbf{P}_i^k\}$ recursively by the following refinement equations

$$\mathbf{P}_i^{k+1} = \sum_{j \in \mathbb{Z}} a_{i-2j} \mathbf{P}_j^k, \quad i \in \mathbb{Z}, \quad k \geq 0. \tag{1}$$

A typical example of a binary subdivision scheme is provided by schemes generating uniform B-splines of order n. In such a case, the mask $\{a_j\}$ is given by $a_j = \frac{1}{2^{n-1}} \binom{n}{j}, j \in \mathbb{Z}$. Some fast scale-space algorithms [2], [3], [4], [5] are, in fact, based on this stationary scheme.

The scheme (1) is called a stepwise interpolatory scheme if and only if the masks $\{a_j, j \in \mathbb{Z}\}$ satisfy $a_{2i} = \delta_i, \forall i \in \mathbb{Z}$. Equation (1) shows clearly that the scheme is a 2-step subdivision scheme. This definition means that one can generate a curve by successive refinements from one resolution level k to the next resolution level $k+1$ in such a way that the points $\{\mathbf{P}_i^k\}$ are kept fixed, while more mid-points are inserted by the interpolation.

2.2 Examples of the Interpolatory Subdivision Scheme

Two simple examples of interpolatory subdivision algorithms are given below.

Example 1. Using w to denote the tension parameter, the "4-point interpolatory scheme" [8], [9] is defined as follows:

$$\begin{cases} \mathbf{P}_{2i}^{k+1} & = \quad \mathbf{P}_i^k, \\ \mathbf{P}_{2i+1}^{k+1} & = \quad (\frac{1}{2} + w)(\mathbf{P}_i^k + \mathbf{P}_{i+1}^k) - w(\mathbf{P}_{i-1}^k + \mathbf{P}_{i+2}^k). \end{cases} \tag{2}$$

It was shown that this scheme produces a C^0 interpolatory curve provided the tension parameter w satisfies $-\frac{1}{2} < w < \frac{1}{2}$ and the curve is also C^1 if $0 < w < \frac{\sqrt{5}-1}{8}$. However, in general the limit curve is not twice differentiable at any point [7], [8], [9].

Example 2. Denoting by s the tension parameter, the following "6-point interpolatory scheme" is studied in [10]:

$$\begin{cases} \mathbf{P}_{2i}^{k+1} & = \quad \mathbf{P}_i^k, \\ \mathbf{P}_{2i+1}^{k+1} & = \quad (\dfrac{9}{16} + 2s)(\mathbf{P}_i^k + \mathbf{P}_{i+1}^k) - (\dfrac{1}{16} + 3s)(\mathbf{P}_{i-1}^k + \mathbf{P}_{i+2}^k) \\ & \quad + s(\mathbf{P}_{i-2}^k + \mathbf{P}_{i+3}^k). \end{cases} \tag{3}$$

It was shown that this scheme produces C^2 interpolatory curves provided the tension parameter s is a small positive number, for example, it suffices if $0 < s < \frac{3}{256}$.

From these two examples and the general subdivision algorithms in [7] and [8], the following symmetric interpolatory subdivision algorithm for curves was investigated [10], [17]:

- *Y.P. Wang was with the Wavelets Strategic Research Programme, National University of Singapore, Singapore 119260. He is now with the Washington University Medical School, St. Louis, MO 63110. E-mail: wyp@cauchy.wustl.edu.*
- *R. Qu is with SDRC-Imageware Inc., Ann Arbor, MI 48105. E-mail: rqu@iware.com.*

Manuscript received 14 Nov. 1998; revised 29 June 1999.
Recommended for acceptance by V.S. Nalwa.
For information on obtaining reprints of this article, please send e-mail to: tpami@computer.org, and reference IEEECS Log Number 107789.

$$\begin{cases} \mathbf{P}_{2i}^{k+1} &= \mathbf{P}_i^k, \\ \mathbf{P}_{2i+1}^{k+1} &= \sum_{j=0}^{n} L_{n,j}(\mathbf{P}_{i-j}^{k+1} + \mathbf{P}_{i+j+1}^{k+1}), \end{cases} \tag{4}$$

where n is called the degree of the scheme and the coefficients $\{L_{n,j}\}$ are chosen to be

$$L_{n,j} = \frac{[(2n+1)!!]^2}{2 \cdot 4^n \cdot (2n+1)!} \cdot \frac{(-1)^j}{2j+1} \cdot \binom{2n+1}{n-j}, \quad j = 0, 1, \cdots, n,$$

where

$$\binom{2n+1}{n-j}$$

denotes the binomial coefficient,

$$(2n+1)!! = (2n+1) \cdot (2n-1) \cdots 3 \cdot 1,$$

$(2n+1)! = (2n+1) \cdot (2n) \cdots 2 \cdot 1$. The sum of the coefficients $\{L_{n,j}\}$ is 1. The following theorem (cf. [10], [17]) is the main convergence and regularity result of scheme (4).

Theorem 1. *The scheme defined by (4) produces $C^{\frac{n}{2}}$ curves for general initial data. Furthermore, for this choice of the coefficients, the scheme reproduces all parametric polynomial curves of degree less than or equal to $2n+1$.*

This theorem shows that the subdivision scheme (4) produces smooth curves and that the choice of the filter coefficients $\{L_{n,j}\}$ gives higher order of approximations. In order to understand the definitions of convergence and smoothness of the subdivision scheme, we first parameterize the curve. As in [7], [8], [9], [10], [17], the dyadic parameterization of a curve means that, at lever $k \geq 0$, the control point $\mathbf{P}_i^k$ is parameterized at the *dyadic points*, $2^{-k}i$, $\forall\, i \in \mathbb{Z}$, in the parameter axis, the t axis. If we define $t_i^k := 2^{-k}i, \forall i \in \mathbb{Z}, k \geq 0,$, then the control polygon $\{\mathbf{P}_i^k,\ i \in \mathbb{Z}\}$ at level k can be regarded as the unique piecewise linear interpolant $\mathbf{P}^k(t)$ from the uniform partition $\cdots t_{-1}^k, t_0^k, t_1^k, \cdots$ of t axis to $\mathbf{R}^3$ satisfying $\mathbf{P}^k(t_i^k) = \mathbf{P}_i^k, i \in \mathbb{Z}$. Hence, the convergence of the scheme can be defined as the convergence of the continuous curve sequence $\{\mathbf{P}^k(t)\}$. We say the scheme is C^m convergent (C^m scheme) if, for any initial data, there is a continuous C^m curve $\mathbf{P}(t)$ such that

$$\lim_{k \to \infty} \mathbf{P}^k(t) = \mathbf{P}(t), \qquad \forall t \in \mathbf{R}.$$

Let $\phi_n(t)$ be the limit curve generated by (4) from the cardinal data $\{\mathbf{P}_i = (i, \delta_0)^T\}$, that is, $\phi_n(t)$ is the fundamental solution of the subdivision scheme (4), then $\phi(i) = \delta_i, i \in \mathbb{Z}$. Furthermore, ϕ_n satisfies the following two-scale relation:

$$\phi_n(t) = \phi_n(2t) + \sum_{j=0}^{n} L_{n,j}\phi_n(2t \pm (2j+1)), \quad t \in \mathbf{R}. \tag{5}$$

Usually, ϕ_n is called the *fundamental function*. If we define the space $V_j = \{\sum_j c_j \phi_n(t-j), t \in \mathbf{R}\}$, (5) will define the multiresolution sampling spaces $\{V_j, j \in \mathbb{Z}\}$ in the following sense:

$$V_j \subset V_{j+1}, \quad j \in \mathbb{Z}. \tag{6}$$

The fundamental function ϕ_n is a very good approximation to the cardinal spline function of order $2n+2$. However, a big difference between them lies in the compactness of supports. Both of them approach the $sinc$ function as n goes to infinity, which is discussed in Section 5.

2.3 Derivatives of the Interpolatory Fundamental Function

In many visual computations, such as the edge detection, optical flow estimation, and curvature estimation, differential operations are usually needed [4]. In this section, a principle is presented for the computation of derivatives of the interpolatory fundamental function ϕ_n at integers. As an example, only the case $n = 2$ is considered. More formulae of numerical differentiation can be found in [11], [16].

From the construction of the algorithm, we know that ϕ_n is an even function and its derivatives can be obtained by the divided difference approximations. Using a local iteration technique, it can be shown that the iteration matrix is given by

$$\begin{pmatrix} 0 & 0 & 1 & 0 & 0 & 0 & 0 & 0 & 0 \\ \frac{3}{256} & -\frac{25}{256} & \frac{150}{256} & \frac{150}{256} & -\frac{25}{256} & \frac{3}{256} & 0 & 0 & 0 \\ 0 & 0 & 0 & 1 & 0 & 0 & 0 & 0 & 0 \\ 0 & \frac{3}{256} & -\frac{25}{256} & \frac{150}{256} & \frac{150}{256} & -\frac{25}{256} & \frac{3}{256} & 0 & 0 \\ 0 & 0 & 0 & 0 & 1 & 0 & 0 & 0 & 0 \\ 0 & 0 & \frac{3}{256} & -\frac{25}{256} & \frac{150}{256} & \frac{150}{256} & -\frac{25}{256} & \frac{3}{256} & 0 \\ 0 & 0 & 0 & 0 & 0 & 1 & 0 & 0 & 0 \\ 0 & 0 & 0 & \frac{3}{256} & -\frac{25}{256} & \frac{150}{256} & \frac{150}{256} & -\frac{25}{256} & \frac{3}{256} \\ 0 & 0 & 0 & 0 & 0 & 0 & 1 & 0 & 0 \end{pmatrix}$$

It can be shown from the property of reproduction of quintic polynomials that the first six eigenvalues and their corresponding eigenvectors of the iterative matrix are

$$\lambda_k = 2^{-k},$$
$$\xi_k = ((-4)^k, (-3)^k, (-2)^k, (-1)^k, 0, 1, 2^k, 3^k, 4^k)^T,$$
$$k = 0, 1, 2, 3, 4, 5.$$

In fact, all the eigenvalues of this matrix are given by

$$1, \frac{1}{2}, \frac{1}{4}, \frac{9}{64}, \frac{1}{8}, -\frac{9}{128}, \frac{1}{16}, -\frac{1}{16}, \frac{1}{32},$$

and the exact values of all the corresponding normalized left and right eigenvectors can be obtained by using *Maple*. For example, the first three pairs are given by:

$$\xi_0 := (1, 1, 1, 1, 1, 1, 1, 1, 1)^T,$$
$$\eta_0 := (0, 0, 0, 0, 1, 0, 0, 0, 0)^T,$$
$$\xi_1 := (-4, -3, -2, -1, 0, 1, 2, 3, 4)^T,$$
$$\eta_1 := (-3, -128, 1272, -6528, 0, 6528, -1272, 128, 3)^T/8760,$$
$$\xi_2 := (16, 9, 4, 1, 0, 1, 4, 9, 16)^T,$$
$$\eta_2 := (9, 192, -1472, 5696, -8850, 5696, -1427, 192, 9)^T/3360.$$

In [11], it was shown, given a square matrix $\mathbf{A}$ of order l, let the normalized left and right (generalized) eigenvectors of $\mathbf{A}$ be denoted by $\{\eta_i, \zeta_i\}$, then for $\forall \mathbf{f} \in \mathbf{R}^l$, one can have the following expansion:

$$\mathbf{f} = \sum_{i=1}^{l} (\mathbf{f}^T \eta_i)\zeta_i. \tag{7}$$

Then, using the divided difference approximation, we have the following:

Theorem 2. *The fundamental solution ϕ_2 is twice continuously differentiable and supported on $[-5, 5]$ and its first and second order derivatives at integers are given by*

$$\phi_2'(i) = \mp sign(i) e_{|i|}^T \eta_1, \quad \phi_2(i) = e_{|i|}^T \eta_2, \quad -4 \leq i \leq 4,$$

where

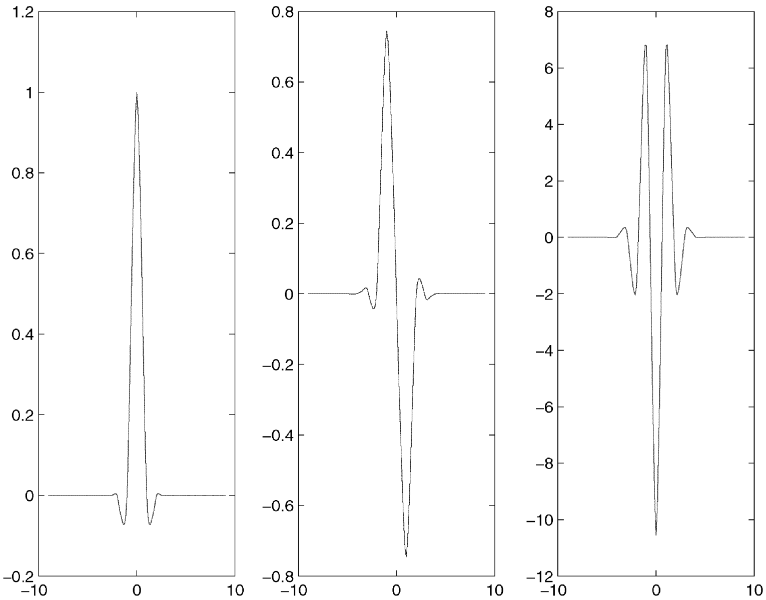

Fig. 1. One-dimensional interpolatory fundamental function ϕ_n and its derivatives ϕ'_n and ϕ''_n for $n = 3$.

$$
\begin{aligned}
e_0 &:= (0,0,0,0,1,0,0,0,0)^T,\\
e_1 &:= (0,0,0,1,0,0,0,0,0)^T,\\
e_2 &:= (0,0,1,0,0,0,0,0,0)^T,\\
e_3 &:= (0,1,0,0,0,0,0,0,0)^T,\\
e_4 &:= (1,0,0,0,0,0,0,0,0)^T.
\end{aligned}
$$

More precisely, we have

$$
\begin{aligned}
\phi'_2(0) &= 0, & \phi''_2(0) &= -\tfrac{295}{56},\\
\phi'_2(\pm 1) &= \mp\tfrac{272}{365}, & \phi''_2(\pm 1) &= \tfrac{356}{105},\\
\phi'_2(\pm 2) &= \pm\tfrac{53}{365}, & \phi''_2(\pm 2) &= -\tfrac{1427}{1680},\\
\phi'_2(\pm 3) &= \mp\tfrac{16}{1095}, & \phi''_2(\pm 3) &= \tfrac{4}{35},\\
\phi'_2(\pm 4) &= \mp\tfrac{1}{2920}, & \phi''_2(\pm 4) &= \tfrac{3}{560}.
\end{aligned}
\tag{8}
$$

Higher order derivatives can be found in [16]. It is easy to show that the derivatives also satisfy a two-scale relation similar to (5). Therefore, from the values at integers, we can compute their values at any dyadic point easily. In Fig. 1, the 1D fundamental function and its first and second order of derivatives are shown for $n = 3$.

3 Fast Algorithm for Scale-Space Filtering Using ISS

3.1 Derivation of the Algorithm

Without loss of generality, suppose N is the number of signal samples and the sampling rate is 1. By the convergence of the subdivision scheme guaranteed by Theorem 1 and the multiresolution property (6), we can represent the signal f at a certain resolution as

$$f(t) = \sum_{i\in\mathbb{Z}} f(i)\phi_n(t-i). \tag{9}$$

A general scale-space filtering approach is defined as the convolution of the signal f with the window function φ with different resolution or scale level s. For feature extraction applications, higher order derivatives are usually needed to describe the geometric structure of an image. Thus, we define the following general operation in scale-space representation explicitly,

$$W_s f(t) = f * \varphi_s^{(m)}(t) = \int f(t-x)\varphi^{(m)}(x)dx, \tag{10}$$

where m denotes the mth order derivative of the window function and $\varphi_s^{(m)}(t) = \varphi^{(m)}(\frac{t}{s})$ is the dilated version of the window $\varphi^{(m)}(t)$. We also approximate the window function φ and its derivatives using the same interpolatory fundamental function:

$$\varphi^{(m)}(t) = \sum_{k\in\mathbb{Z}} \varphi(i)\phi_n^{(m)}(t-i), \quad m = 0,1,2,\cdots. \tag{11}$$

Since any scale s can be represented as $s = 2^l a, l \in \mathbb{Z}$, where a controls the number of the initial sampling points, we only consider the dyadic scale case and assume $a = 1$ throughout the paper.

Substituting (9), (11) into (10), we obtain

$$
\begin{aligned}
W_{2^l} f(t) &= \Big(\sum_{i\in\mathbb{Z}} f(i)\phi_n(t-i)\Big) * \Big(\sum_{k\in\mathbb{Z}} \varphi(k)\phi_n^{(m)}(2^{-l}t-k)\Big)\\
&= \sum_i\sum_k f(i)\varphi(k)(\phi_n(t-i) * \phi_n^{(m)}(2^{-l}t-k)).
\end{aligned}
\tag{12}
$$

Due to the two-scale relation (5), it can be concluded that the derivatives of the fundamental function satisfy the following two-scale relation

$$\frac{1}{2^m}\phi_n^{(m)}\Big(\frac{t}{2}\Big) = \phi_n^{(m)}(t) + \sum_{j=0}^{n} L_{n,j}\phi_n^{(m)}(t \pm (2j+1)), \quad t \in \mathbf{R}. \tag{13}$$

For simplicity, we can express (13) in the following form:

$$\phi_n^{(m)}\Big(\frac{t}{2}\Big) = [M * \phi_n^{(m)}](t), \tag{14}$$

where the mask or transfer function M is given by the following sequence:

$$M := 2^m\{L_{n,n}, 0, L_{n,n-1}, \cdots, 0, L_{n,0}, 1, L_{n,0}, 0, \cdots, L_{n,n-1}, 0, L_{n,n}\}.$$

Therefore, (13) can be rewritten as:

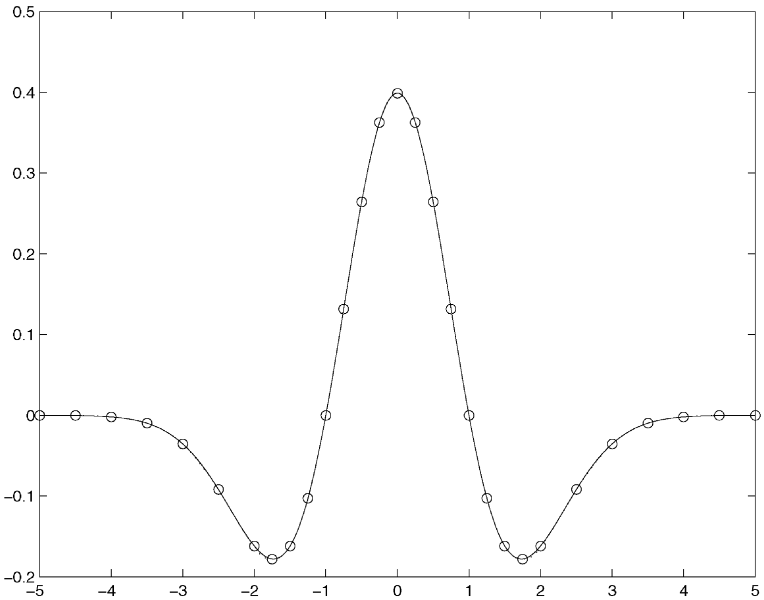

Fig. 2. Approximation to the Mexican hat operator using the ISS. The number of the interpolation points is 29. After four iterations, the number of interpolating points is 225, which are shown by the solid line. The theoretical curve is shown by the dotted line. The approximation error is 7.1278e-05.

$$\begin{aligned}\phi_n^{(m)}(2^{-l}t-k) &= \phi_n^{(m)}(\frac{1}{2}(2^{-l+1}t-2k)) \\ &= [M*\phi_n^{(m)}](2^{-l+1}t-2k) \\ &= \cdots = [\overbrace{M*M_{\uparrow 2}*\cdots *M_{\uparrow 2^{l-1}}}^{l}*\phi_n^{(m)}](t-2^l k),\end{aligned}$$

where $\uparrow 2^{l-1}$ represents the up-sampling operation of the filter M, i.e., between every two adjacent samples of the filter $2^{l-1}-1$ zeros are inserted. Therefore, for this type of convolution, the complexity is the same as that of the convolution with the filter M. It follows that:

$$\begin{aligned}&\phi_n(t-i)*\phi_n^{(m)}(2^{-l}t-k) = \\ &[\phi_n*\phi_n^{(m)}*\overbrace{M*M_{\uparrow 2}\cdots *M_{\uparrow 2^{l-1}}}^{l}](t-i-2^l k).\end{aligned}$$

We now can express (12) as:

$$\begin{aligned}W_{2^l}f(t) &= \sum_i\sum_k f(i)\varphi(k)[\phi_n*\phi_n^{(m)}*\overbrace{M*M_{\uparrow 2}*\cdots *M_{\uparrow 2^{l-1}}}^{l}] \\ &\quad (t-i-2^l k) \\ &= [f*\overbrace{M*M_{\uparrow 2}*\cdots *M_{\uparrow 2^{l-1}}}^{l}*\phi_n*\phi_n^{(m)}*\varphi_{\uparrow 2^l}](t).\end{aligned} \tag{15}$$

By taking $t=j, j\in\mathbb{Z}$, we only need to compute the values

$$c(j) = [\phi_n*\phi_n^{(m)}](j) = \int_{-\infty}^{\infty}\phi_n(j-t)\phi_n^{(m)}(t)dt, \quad j\in\mathbb{Z}. \tag{16}$$

As discussed in Section 2, the values of ϕ_n and $\phi_n^{(m)}$ at the dyadic points can be exactly computed. Hence, the value of $c(j)$ can be computed numerically to sufficient accuracy. Moreover, due to the compact support property of ϕ_n and $\phi_n^{(m)}$, we have a finite number of nonzero values of $c(j)$. Then, these values are stored in a table for fast computations. The implementation steps are summarized below.

$$\begin{array}{llll} Scale\ 1: & S_1f = f*c, & W_1f = S_1f*\varphi, & \\ Scale\ 2: & S_2f = S_1f*M, & W_2f = S_2f*\varphi_{\uparrow 2}, & \\ Scale\ 2^j: & S_{2^j}f = S_{2^{j-1}}f*M_{2^{j-1}}, & W_{2^j}f = S_{2^j}f*\varphi_{\uparrow 2^j}, & 2\le j\le J. \end{array} \tag{17}$$

3.1.1 Complexity Analysis

In the above formula, the long convolution is factored into a series of small convolutions. One can compute the scale-space filtering at the coarse scale 2^l from the fine scale 2^{l-1} by convolution with the mask $M_{2^{l-1}}$. At each iteration, the number of multiplications is $\mathcal{O}(N)$. So, for J scales, the complexity becomes $\mathcal{O}(JN)$, if, by direct convolution, the complexity at scale J is $\mathcal{O}(2^J N)$, which increases very fast with the scale J.

3.2 Approximation Error Analysis

In the previous section, both the signal f and the window filter $\varphi_n^{(m)}$ are projected into the multiresolution sampling spaces. Now, we study its approximation errors.

Error estimates of the approximation to the limit curve by the piecewise linear interpolant $\mathbf{P}^k(t)$ are given below. It is shown that the scheme (5) has the approximation power of $\mathcal{O}(h^{2n+2})$. It is also shown that the approximation is simultaneous with their derivatives. For details, see [11], [17].

Theorem 3. *Suppose $\mathbf{F}(t),\ t\in\mathbf{R}$, is a regular and C^{2n+2} curve in $\mathbf{R}^m$, $m\ge 2$. Let $\mathbf{P}(t),\ t\in\mathbf{R}$ be the limit curve generated by scheme (4) from the initial data $\mathbf{P}_i := F(ih),\ i\in\mathbb{Z},\ 0<h<1$. Then, on any finite interval $[a,b]$, we have the following estimate*

$$\|\mathbf{F}(ht)-\mathbf{P}(t)\|_\infty \le \frac{M_{2n+2}(\mathbf{F})}{(2n+2)!}h^{2n+2} = \mathcal{O}(h^{2n+2}),$$

where $M_{2n+2}(\mathbf{F})$ depends only on the derivatives of $\mathbf{F}(t)$ and n. For the derivative case, we also have

$$\|h^m\mathbf{F}^{(m)}(ht)-\mathbf{P}^{(m)}(t)\|_\infty = \mathcal{O}(h^{2n+2-m}), \quad m=0,1,2,\cdots\frac{n}{2}.$$

From these results, the approximation error of computing the scale-space filtering can be obtained:

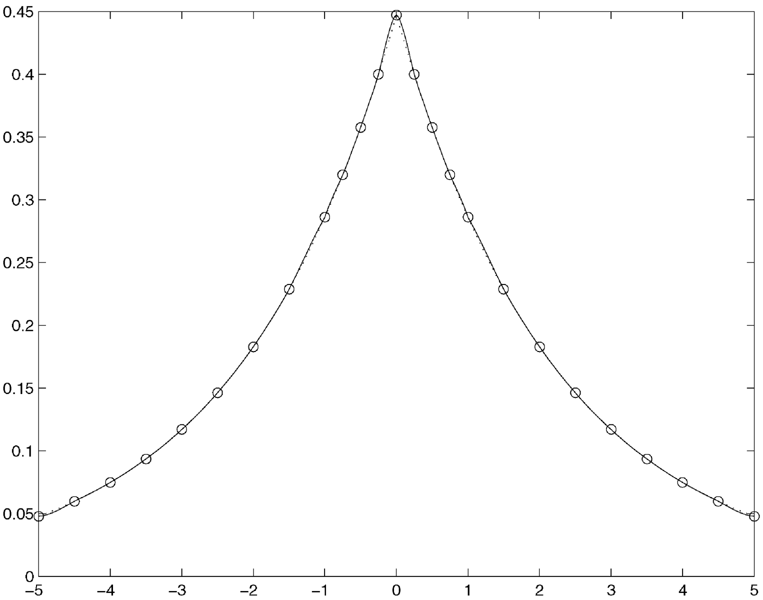

Fig. 3. Approximation to the first-order R-filter in [12] using the ISS. The number of the interpolation points is 25. Near the origin, more interpolation points are used. After three iterations, the number of interpolating points is 193, which are shown by the solid line. The theoretical curve is shown by the dotted line. The approximation error is 4.6562e-04.

$$\begin{aligned}\|W_{2^l}f - \tilde{W}_{2^l}f\|_\infty &= \|f * \varphi_{2^l}^{(m)} - \tilde{f} * \tilde{\varphi}_{2^l}^{(m)}\|_\infty \\ &\leq \|f - \tilde{f}\|_\infty \|\varphi^{(m)}\|_\infty + \|\varphi_{2^l}^{(m)} - \tilde{\varphi}_{2^l}^{(m)}\|_\infty \|\tilde{f}\|_\infty.\end{aligned}$$

Thus, the approximation order of fast scale-space filtering algorithm (15) is $\mathcal{O}(h^{2n+2-m})$.

4 Implementation Examples

In low level image processing, there are a number of high-performance edge detection operators, such as the LoG operator [13], the Canny detector [14], the first-and-second order R-filters, Deriche's detector, Sarkar and Boyer's detector, and Shen and Castan's edge detectors [12]. Generally, these filters are special instances of the generalized edge detectors proposed by Gökmen and Jain [12] for $\lambda\tau$-space representation of images, where λ controls the scale of the filter and τ controls the shape of the filter. There remain urgent problems for the efficient realization of these filters. For such a representation when τ is small, there is a strong discontinuity at the origin. Using the ISS approach, more interpolation points can be assigned around this region. For illustrative purposes, the interpolation results are demonstrated in the following two examples, where the order of the subdivision scheme is 2.

The first one is the famous Marr-Hildreth operator [13], which is the second order derivative of the Gaussian kernel:

$$G(x;\lambda) = \frac{1}{\sqrt{2\pi}\lambda}(1-x^2)exp(-\frac{x^2}{2\lambda^2}). \tag{18}$$

The other is the first-order R-filter (cf. [12]):

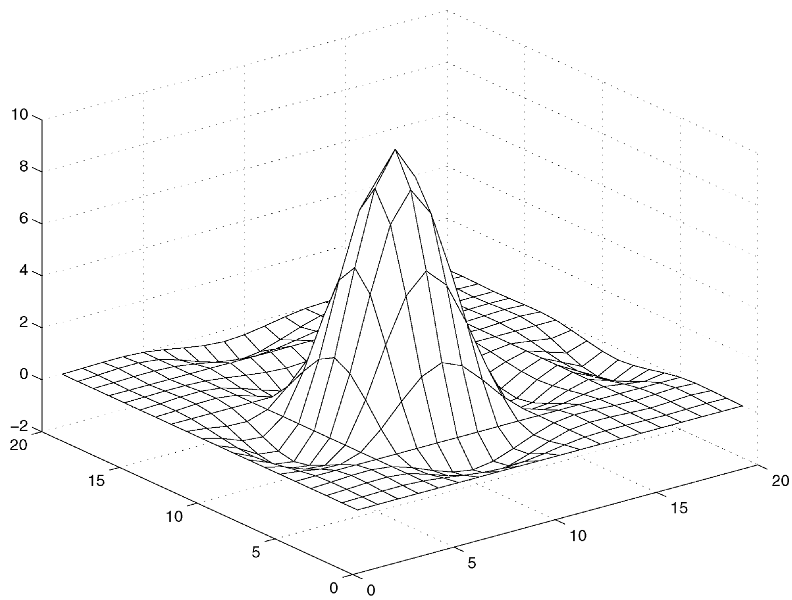

Fig. 4. Two-dimensional interpolatory fundamental function $\phi_3(x)\phi_3(y)$.

Fig. 5. Comparison with different interpolation techniques. Top left: nearest neighbor interpolation. Top right: bilinear interpolation. Bottom left: cubic spline interpolation. Bottom right: interpolatory subdivision scheme.

$$R_1(x,\lambda) = \frac{1}{2\lambda} exp(-\frac{|x|}{\lambda}). \tag{19}$$

As shown in Figs. 2 and 3, the approximation results are very good. The approximation error is measured in the l^2 norm. The quality of the approximation increases with the number of selected interpolation points. Furthermore, the interpolation is local so that we can assign more points in the area with more oscillations, as shown in Fig. 3.

4.1 Extension to 2D

The 1D method can be extended directly to 2D case using tensor product. Fig. 4 shows the 2D fundamental function. We also compare the interpolation results in Fig. 5 between the different interpolation technologies, such as the nearest neighbor interpolation, the bilinear interpolation, and the cubic spline interpolation. It is clear that the ISS is superior to both the nearest neighbor and the bilinear interpolations. It is hard to tell the difference between the cubic spline interpolation and ISS visually. But, the ISS technique is more efficient since it does not solve any linear system.

5 Discussions

5.1 Relation with the Whittaker-Shannon Sampling Theorem

In the derivation of our algorithm, the interpolatory basis function ϕ_n is used for multiresolution interpolation. It is therefore necessary to establish its relation with the standard sampling theorem, which states that a band-limited signal can be recovered from its discrete samples using *sinc* bases. For this purpose, we study the asymptotic behavior of the subdivision scheme (4) when the order n tends to infinity.

First, it can be shown that

$$\lim_{n\to\infty} L_{n,j} = \frac{1}{\pi}\frac{(-1)^j}{2j+1}. \tag{20}$$

Since

$$\begin{aligned} L_{n,j} &= \frac{[(2n+1)!!]^2}{2\cdot 4^n\cdot(2n+1)!}\frac{(-1)^j}{2j+1}\binom{2n+1}{n-j} \\ &= \frac{(-1)^j}{2j+1}\frac{[(2n+1)!!]^2}{2\cdot 2^{2n}\cdot(n+1)!n!}\prod_{k=1}^{j+1}\frac{n-k+1}{n+k}\frac{n+1}{n-j}, \end{aligned}$$

and

$$\lim_{n\to\infty}\prod_{k=1}^{j+1}\frac{n-k+1}{n+k}\frac{n+1}{n-j} = 1,$$

we need only to consider the limit of the term

$$A(n) := \frac{[(2n+1)!!]^2}{2\cdot 2^{2n}\cdot(n+1)!n!} = \frac{[(2n+1)!]^2}{2^{4n+1}(n+1)(n!)^4},$$

where $(2n+1)!! = \frac{(2n+1)!}{(2n)!!} = \frac{(2n+1)!}{2^n(n)!}$ is used. From Stirling's formula,

$$\lim_{n\to\infty} \frac{n!}{\sqrt{2\pi} n^{n+\frac{1}{2}} e^{-n}} = 1,$$

it follows that

$$\begin{aligned}\lim_{n\to\infty} A(n) &= \lim_{n\to\infty} \frac{[\sqrt{2\pi}(2n+1)^{\frac{2n+1+1}{2}} e^{-(2n+1)}]^2}{2^{4n+1}(n+1)(\sqrt{2\pi} n^{\frac{n+1}{2}} e^{-n})^4} \\ &= \lim_{n\to\infty} \frac{1}{\pi} \frac{2n}{n+1} [(1+\frac{1}{2n})^{2n}]^2 (1+\frac{1}{2n})^3 e^{-2} \\ &= \frac{2}{\pi}.\end{aligned}$$

Therefore, we have

$$\lim_{n\to\infty} L_{n,j} = \frac{1}{\pi} \frac{(-1)^j}{2j+1}, \quad j \in \mathbb{Z}.$$

Thus, the filter response $h^{\infty}(k)$ in the two-scale relation (5) at infinity becomes:

$$h^{\infty}(k) = \begin{cases} \delta_j & for \quad k = 2j, \\ L_{\infty,j} & for \quad k = 2j+1 \end{cases} = \frac{sin\frac{k\pi}{2}}{\frac{k\pi}{2}}, \tag{21}$$

and the interpolatory function ϕ_n approaches the $sinc$ function $\phi_{\infty}(t) = \frac{sin\pi t}{\pi t}$ as n increases. This result indicates that, for a bandlimited signal and a fixed resolution, we can increase the length of $L_{n,j}$ to improve the approximation accuracy. However, this is not necessary since a large filter size will decrease the computational efficiency. One may notice that the fundamental spline also possesses this property when its order tends to infinity.

5.2 Comparison with the Fundamental Spline Method

The B-spline method has been widely used for efficient implementations of scale-space filtering, in particular for linear Gaussian scale-spaces. One of its properties is good approximation to the Gaussian function. As a result, it is suitable for approximating Marr-Hildreth and Canny operators [2], [4], [5]. As we have mentioned before, the B-spline approach is one type of subdivision schemes. However, this basis function is not interpolatory. One possible alternative is to use the fundamental or cardinal splines. However, since a fundamental spline function has an infinite support, one has to truncate an infinite filter sequence or use other approximation techniques [3], [2]. For ISS, the fundamental function has a compact support. Moreover, one can select the interpolation points nonuniformly. This is very suitable to approximate certain types of edge detection filters in [12], which have large curvature values at the origin. One can assign more interpolation points at these locations. The disadvantage of ISS is that the computational speed is a little slower than that of the spline approach which involves mostly the addition operation [4], [5] and the generated curve is not a polynomial spline.

6 CONCLUSIONS

The efficient implementation of scale-space filtering is very important in practice. Various techniques have been used for this purpose. In this paper, the ISS method is introduced for high performance computation. We consider various issues such as the computation of derivatives of interpolating functions and the approximation errors. In view of the sampling theorem, the ISS can be regarded as the multiresolution approximation of a signal with the interpolating basis function of compact support, which is superior to the standard $sinc$ function. The ISS reproduces certain polynomials. More importantly, it has certain data-dependent shape preserving properties. Therefore, it is suitable for approximating filters like the generalized edge detection filters discussed in [12], which have arbitrary shapes.

ACKNOWLEDGMENTS

This work is supported by the Wavelets Strategic Research Programme funded by the National Science and Technology Board and Ministry of Education of Singapore under Grant RP960 601/A.

REFERENCES

[1] A.P. Witkin, "Scale-Space Filtering," *Proc. Seventh Joint Conf. Artificial Intelligence,* pp. 1,019-1,023 Karlsruhe, W. Germany, 1983.
[2] L.A. Ferrari, P.V. Sankar, S. Shinnaka, and J. Sklansky, "Recursive Algorithms for Implementing Digital Image Filters," *IEEE Trans. Pattern Analysis and Machine Intelligence,* vol. 9, no. 3, pp. 461-466, 1987.
[3] M. Unser, A. Aldroubi, and M. Eden, "B-Spline Signal Processing: Part 1—Theory," *IEEE Trans. Signal Processing,* vol. 41, no. 2, pp. 821-833, 1993.
[4] Y.-P. Wang, "Image Representations Using Multiscale Differential Operators," *IEEE Trans. Image Processing,* to appear, available at http://wavelets.math.nus.edu.sg/~wyp/download_papers/Edgespline.ps.gz.
[5] Y.-P. Wang, S.L. Lee, "Scale-Space Derived from B-Splines," *IEEE Trans. Pattern Analysis and Machine Intelligence,* vol. 20, no. 10, pp. 1,040-1,055, Oct. 1998.
[6] I. Daubechies, "Orthonormal Bases of Compactly Supported Wavelets," *Comm. Pure Appl. Math.,* vol. XLI, pp. 909-996, 1988.
[7] A. Cavaretta, C. Micchelli, and W. Dahmen, "Stationary Subdivision," *AMS Memoirs,* vol. 93, no. 453, 1991.
[8] S. Dubuc, "Interpolation through an Iterative Scheme," *J. Math. Analysis and Applications,* vol. 144, pp. 185-204, 1986.
[9] N. Dyn, J.A. Gregory, and D. Levin, "A 4-Point Interpolatory Subdivision Scheme for Curve Design," *Computer Aided Geometric Design,* vol. 4, pp. 257-268, 1987.
[10] R. Qu, "Curve and Surface Interpolation by Subdivision Algorithms," *Computer Aided Drafting, Design, and Manufacturing,* vol. 4, no. 2, pp. 28-39, 1994.
[11] R. Qu and R.P. Agarwal, "Solving Two Point Boundary Value Problems by Interpolatory Subdivision Algorithms," *Int'l J. Computer Math.,* vol. 60, pp. 279-294. 1996.
[12] M. Gökmen and A.K. Jain, "$\lambda\tau$-Space Representation of Images and Generalized Edge Detector," *IEEE Trans. Pattern Analysis and Machine Intelligence,* vol. 19, no. 6, pp. 545-563, June 1997.
[13] D. Marr and E. Hildreth, "Theory of Edge Detection," *Proc. Royal Soc. London,* vol. B207, pp. 187-217, 1980.
[14] J. Canny, "A Computational Approach to Edge Detection," *IEEE Trans. Pattern Analysis and Machine Intelligence,* vol. 8, no. 1, pp. 679-698, 1986.
[15] R. Deriche, "Optimal Edge Detection Using Recursive Filtering," *Proc. IEEE First Int'l Conf. Computer Vision,* pp. 501-505, London, 1987.
[16] R. Qu, "A New Approach to Numerical Differentiation and Integration," *Math. Comput. Modeling,* vol. 24, no. 10, pp. 55-68, 1996.
[17] R. Qu and R.P. Agarwal, "A Cross Difference Approach to the Analysis of Subdivision Algorithms," *Neural, Parallel & Scientific Computations,* vol. 3, no. 3, pp. 393-416, 1995.